

The high-energy emission from GX 339–4 as seen with INTEGRAL and XMM-Newton

M. D. Caballero-Garcia*†

University of Cambridge, Institute of Astronomy, Cambridge CB3 0HA, UK

E-mail: mcaballe@ast.cam.ac.uk

J. M. Miller

Department of Astronomy, University of Michigan, 500 Church Street, Ann Arbor, USA, MI

48109

E-mail: jonmm@umich.edu

A. C. Fabian

University of Cambridge, Institute of Astronomy, Cambridge CB3 0HA, UK

E-mail: acf@ast.cam.ac.uk

, on behalf of a larger collaboration team.

GX 339–4 is a well-known microquasar. In this contribution we show the obtained results with the INTEGRAL and XMM-Newton observatories of the outburst undertaken on 2007. The observations cover spectral evolution from the hard, soft intermediate states to the high/soft state. Spectral hardening correlated with the appearance of an skewed Fe line is detected during one of the observations during the soft intermediate state. In all spectral states joint XMM/EPIC-pn, JEM-X, ISGRI and SPI data were fit with the hybrid thermal/non-thermal Comptonization model (EQPAIR). With this model a non-thermal component seems to be required by the data in all the observations. Our results imply evolution in the coronal properties, the most important one being the transition from a compact corona in the first observation to the disappearance of coronal material in the second and re-appearance in the third. We discuss the results obtained in the context of possible physical scenarios for the origin and geometry of the corona and its relation to black hole states.

7th INTEGRAL Workshop

September 8-11 2008

Copenhagen, Denmark

*Speaker.

†This work is based on observations made with *INTEGRAL*, an ESA science mission with instruments and science data centre funded by ESA member states and with the participation of Russia and the USA and on observations with *XMM-Newton*, an ESA science mission with instruments and contributions directly funded by ESA member states and the USA (NASA).

1. Black Hole States

When a Black Hole (hereafter BH) transient starts an outburst, it evolves through different states (low/hard, hard intermediate, soft intermediate, high/soft states) characterized by different spectral, timing, optical, IR and radio properties. For a recent prescription of the state classification scheme we refer to [12] and [1]. In the earlier times of this science (before 1990s) it was thought that the state evolution of a black hole was driven by \dot{M} ([5]). But, since some states can span a large variation in luminosities, it was suggested ([11]) that other parameter may play a role in these state transitions. This parameter could be, e.g. the coronal compactness of the high-energy emission.

In the state evolution of most Black Hole Binaries (BHB) ([1], [12]), these start their outbursts in the Low/Hard (LH) state and evolve to the High/Soft (HS) state, passing through Hard Intermediate (HIMS) and Soft InterMediate (SIMS; formerly called Very/High) states and, afterwards, they return to the LH state showing a noticeable decrease in flux of the order of 50%, in a hysteresis behaviour ([21], [24] and [16]; see evolution in Figure 1). In the following, we list some spectral characteristics of all the different states from the recent prescription, apart from the quiescent state in which black hole transients spend most part of their lives.

- Low/hard state (LS): this is the state in which the outbursts begin and end. The X-ray spectrum is characterized by very low disk emission and very important high-energy emission in the form of a powerlaw with photon index in the range $\Gamma = 1.3 - 1.4$. A high-energy cut-off is usually seen ([25] and [10]), associated to the kinetic temperature of the thermal distribution of electrons in the Comptonizing corona. Sometimes, low frequency QPOs are observed. Flat-spectrum radio emission is observed, associated to a compact jet ejection ([6]).
- Intermediate (soft/hard) states (SIMS/HIMS): showing both bright disk and high-energy powerlaw emission components. Photon index is within the range $\Gamma = 1.5 - 2.5$. The few instances of HFQPOs appeared in the SIMS (formerly called as Very/High state). Just before the transition to the SIMS, [6] suggested that the jet velocity increased rapidly, giving rise to a fast relativistic jet.
- High/Soft state (HS): the disk component is the dominant in the spectrum, with a weak powerlaw high-energy emission. No core radio emission is observed ([6]). Some timing properties ([26]), that were thought to be characteristic of the LH and HIMS are still present in this state, although in a much weaker form. This would suggest a common origin in the characteristics found in these states. No high-energy cut-off is observed in this state ([10]).

2. Source of the high-energy emission

The X/ γ -ray spectra (1–1 000 keV) from black holes can be described by a soft disk emission (< 10 keV) plus a high-energy emission (> 20 keV) in the form of a powerlaw. The soft X-ray spectra often shows signatures from the inner parts of the accretion disk, such as the relativistic Fe line (6.4–6.97 keV) and the correspondent reflection bump (20–30 keV), both being different

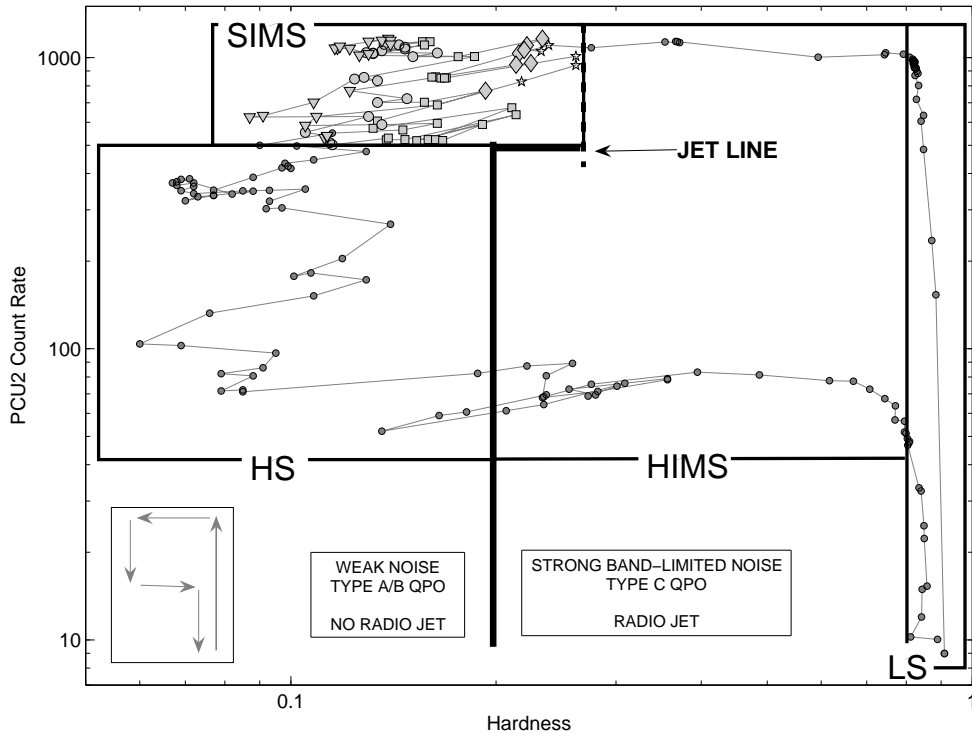


Figure 1: Hardness-Intensity diagram of the 2002/2003 outburst of GX 339–4 as observed by the RXTE PCA. The gray lines mark the state transitions described in the text. The inset on the lower left shows the general time evolution of the outburst along the q -shaped pattern. From [1].

aspects of the same physical origin (i.e. fluorescence of the Fe ions and Compton back-scattering, respectively, both being the most obvious reactions of an irradiated disk by a high-energy source; [8]).

The high-energy emission comes from the (inverse) Comptonization of the soft seed photons from the inner accretion disk by a corona (consituted by electrons and positrons). Both the geometry and location of this corona are a matter of debate. In the former model ([5]), this corona was filling the inner regions of a truncated disk. [18], [19] showed that the base of a jet could replace an extended corona for the high-energy emission source. Independently, [20] found the existence of an inner disk in GX 339–4 during LH state from X-ray observations. All these issues can be better explained if the base of a jet is the source of hard X-ray emission. This scenario is very tempting, due to the non-thermal emission already observed in BHs during different states ([14] in the LH, [17] and [9] in the intermediate and HS states, respectively), which could be understood as, e.g. synchrotron processes occurring at the base of the jet.

We will show in the following that the base of a jet, which evolves in properties (opacity, compacticity and distance from the BH) during the outburst, could give rise to the X/γ properties already observed in the black hole candidate GX 339–4.

Epoch	XMM-Newton ID	INTEGRAL (yyyy/mm/dd)	XMM-Newton (UTC hh:mm ; yyyy/mm/dd)
1	–	2007/01/30-02/01	–
2	0410581201	2007/02/17-19	00:03–04:44 ; 2007/02/19
3	0410581301	2007/03/04-06	11:15–11:15 ; 2007/03/05
4	–	2007/03/16-18	–
5	0410581701	2007/03/29-31	14:34–20:07 ; 2007/03/30

Table 1: *INTEGRAL* and *XMM-Newton* Observations LOG.

Obs. number	ℓ_h/ℓ_s	ℓ_{nth}/ℓ_h	τ_p	kT_e (keV)	$[\Omega/2\pi]$
1	$3.9^{+0.6}_{-0.2}$	$0.40^{+0.15}_{-0.03}$	$2.39^{+0.15}_{-0.18}$	27.5 ± 1.2	$0.38^{+0.06}_{-0.04}$
2	$0.05^{+0.003}_{-0.01}$	0.90 ± 0.10	< 0.02	69 ± 4	$0.40^{+0.3}_{-0.04}$
3	$0.28^{+0.03}_{-0.01}$	0.84 ± 0.03	$1.41^{+0.03}_{-0.06}$	10.8 ± 0.3	1(f)
4	$0.24^{+0.02}_{-0.005}$	$0.49^{+0.02}_{-0.01}$	2.5 ± 0.5	4.3 ± 0.8	1(f)
5	$0.13^{+0.01}_{-0.02}$	0.38 ± 0.02	$0.89^{+0.04}_{-0.05}$	10.5 ± 0.7	$0.72^{+0.16}_{-0.10}$

Table 2: Best-fit parameters of the joint XMM/EPIC-pn, JEM-X, ISGRI and SPI spectra for the 5 obs. Fits have been performed simultaneously with EQPAIR combined with LAOR.

3. *INTEGRAL* and *XMM-Newton* observations of GX 339–4

In [2] we present simultaneous *XMM-Newton* and *INTEGRAL* observations of the luminous black hole transient and relativistic jet source GX 339–4. GX 339–4 started an outburst on November of 2006 and our observations were undertaken from January to March of 2007 (see Table 1). We triggered five *INTEGRAL* and three *XMM-Newton* target of Opportunity observations within this period. Our data cover different spectral states, namely Hard Intermediate (obs. 1), Soft Intermediate (obs. 2 and 3) and High/Soft (obs. 4 and 5).

The hybrid thermal/non-thermal Comptonization EQPAIR model ([3]) provides the injection of a non-thermal electron distribution with Lorentz factors between Γ_{min} and Γ_{max} and a powerlaw spectral index Γ_{inj} . The cloud is illuminated by soft thermal photons emitted by an accretion disk. These photons serve as seed for inverse Compton scattering by both thermal and non-thermal electrons. The system is characterized by the power (i.e. luminosity) L_i supplied by its different components. We express each of them dimensionlessly as a compactness parameter, $\ell_i = L_i \sigma_T / (R m_e c^3)$, where R is the characteristic dimension and σ_T the Thompson cross-section of the plasma. Thus, ℓ_s , ℓ_{th} , ℓ_{nth} and $\ell_h = \ell_{th} + \ell_{nth}$ correspond to the power in a soft disk entering the plasma, thermal electron heating, electron acceleration and the total power supplied to the plasma. The total number

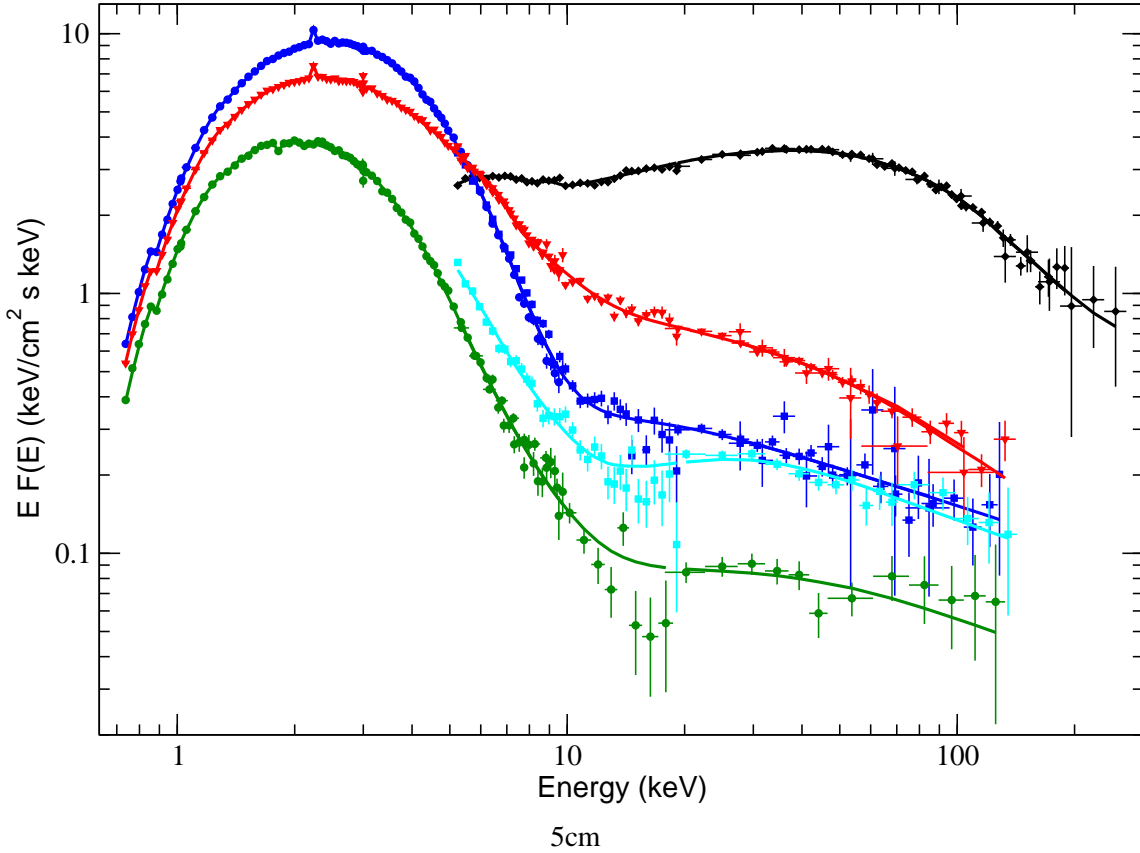


Figure 2: Unfolded spectra from epoch 1 to 5 (black, blue, red, cyan and green, respectively).

of electrons (not including e^+e^- pairs) is determined by τ_T , the corresponding Thompson optical depth, measured from the center to the surface of the scattering region. If we consider injection from pairs e^+e^- , then the total optical depth of the thermalized scattering electrons/pairs is expected to be $\tau_T \geq \tau_p$. We used the LAOR model ([15]) to model the relativistic iron line emission, with the emissivity index (β) free and tied to the opposite value of that of the EQPAIR.

In the EQPAIR model, emission of the disk/corona system is modeled by a spherical hot plasma cloud with continuous acceleration of electrons illuminated by soft seed photons from the accretion disk. At high-energies the distribution of electrons is non-thermal, but at low energies a Maxwellian distribution with temperature kT_e is established.

In general, the spectral shape is insensitive to the exact value of the compactness, but it depends strongly on the compactness ratios (ℓ_h/ℓ_s and ℓ_{nth}/ℓ_h). Thus, we froze ℓ_s to a fiducial value ($\ell_s = 10$), as commonly reported for other sources with similar characteristics (e.g. [13]). In the fits reported below, we fit the data with a powerlaw distributed injection of electrons and compare with the results obtained with a mono-energetic distributed injection of them as well. The former distribution is expected in the case of shock acceleration of particles, while the second could be achieved in reconnection events that are expected to power the corona ([7]).

Spectra and unfolded models of the five different periods have been plotted in Figure 2. In Table 2 we show the evolution of the most important parameters inferred from the model.

The results obtained by applying EQPAIR fits to the data indicate a high value for the coronal compactness for obs. 1, but within the range of values found in the literature. For obs. 3, 4 and 5 this value is high as well (when compared to that obtained in obs. 2). We thus confirm the correlation between coronal compactness and covering fraction of the cold reflecting material by [22] for obs. 2 to 5. The high value of the coronal compactness found for obs. 1 (HIMS) would indicate that the Comptonizing high-energy source is compact in size. This would be in agreement with the proposed scenario of [19], in which the base of the jet could be the source of the Comptonizing electrons. The fact that we are detecting the thermal cut-off would be consistent with the detection of the coronal emission as well. Otherwise, for obs. 2 (SIMS), the values for both the coronal compactness and opacity found are extremely low. Moreover, the kinetic temperature found for the thermal electron distribution of the corona is very high (and close to the high-energy limit indeed). We understand them as issues indicative of the lack of coronal emission during this observation. During obs. 3 to 5 (SIMS to HS), both the coronal compactness and opacity increase again (accompanied with the significant detection of a relativistic line in obs. 3), thus indicating re-appearance of the corona after obs. 2.

We fit the data with a powerlaw distributed injection of accelerated non-thermal electrons (with Lorentz factors in the range of $\Gamma = 1.3 - 100$) and compared with the results obtained with a mono-energetic distributed injection (with Lorentz factor $\Gamma = 5$) of them as well. The former distribution is expected in the case of shock acceleration of particles, while the second could be achieved in reconnection events that are expected to power the corona ([7]). We found that the first model is better than the second for epochs 1, 3, 4 and 5 (applying an F-test and looking at the residuals, i.e. see Table 3 and Figure 3). This is indicative of a corona of particles distributed at different speeds being the source of the high-energy emission. However, for epoch 2, albeit the first proposed scenario is not discarded, and contrary to the remainder epochs, a mono-energetic distribution of particles is a good description of the spectrum. It seems that magnetic reconnection events are driving the high-energy emission in this epoch.

Thus, we conclude that we detect spectral evolution in our data compatible with disappearance of a part ¹ of the corona in epoch 2 (SIMS). This was followed by its re-appearance in epoch 3 (SIMS) and maintained in epochs 4 and 5. Giving strength to this interpretation is the fact that [4] detected a series of plasma ejection events during 4–18 of February (2007) in radio, just previously to our observations of epoch 2. Also, the sudden increase in flux in the 15–50 keV of the SWIFT/BAT light curve (Figure 4) of 15% could be related to changes occurring in the source of the high-energy emission during the transition from epochs 2 to 3. The possible disappearance of the corona during epoch 2 resembles what claimed by [23] in the case of GRS 1915+105. This behavior could be understood as the fact that the ejected medium is the coronal material responsible for the hard X-ray emission. The spectra of epochs 1, 3, 4 and 5 show a significant fraction of non-thermal particles as well, indicating that it could be due to other processes apart from thermal Comptonization. For example, synchrotron or self-synchrotron emission ([18],[19]) occurring at the base of a jet.

¹Since the model still requires a high-energy component.

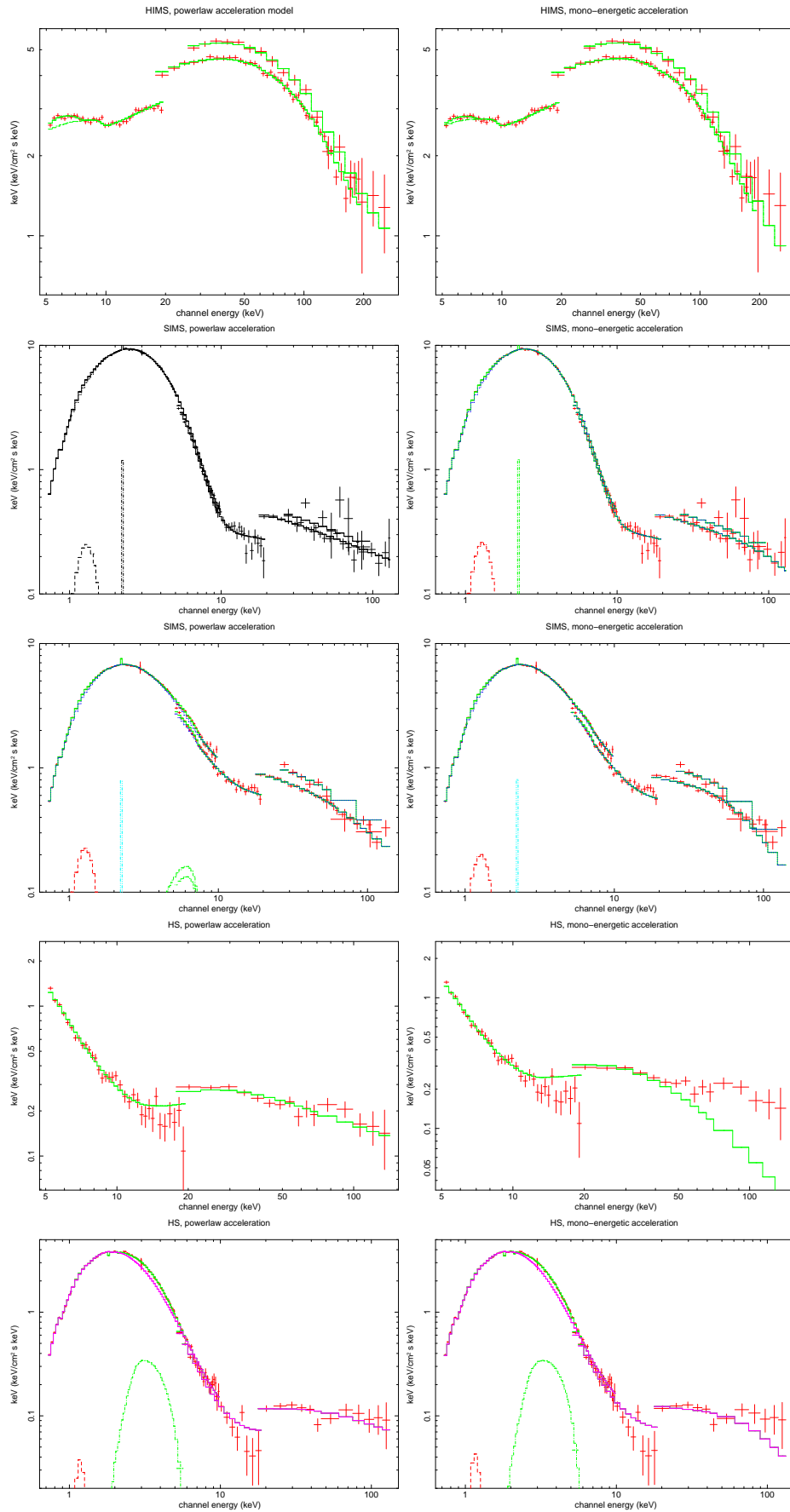


Figure 3: Unfolded spectra from epoch 1 to 5 applying EQPAIR fits to the data with both mono-energetic and powerlaw acceleration cases. The vertical lines represent the different energies used for the different

Epoch	Mono-energetic acceleration (red. chi-square; number of d.o.f.)	Powerlaw acceleration (red. chi-square; number of d.o.f.)	F-test probability
1	1.1 (83)	1.0 (82)	0.003
2	1.7 (143)	1.7 (142)	—
3	1.9 (139)	1.5 (138)	7.1e-09
4	4.5 (45)	1.5 (44)	2.8e-12
5	1.7 (100)	1.6 (99)	0.008

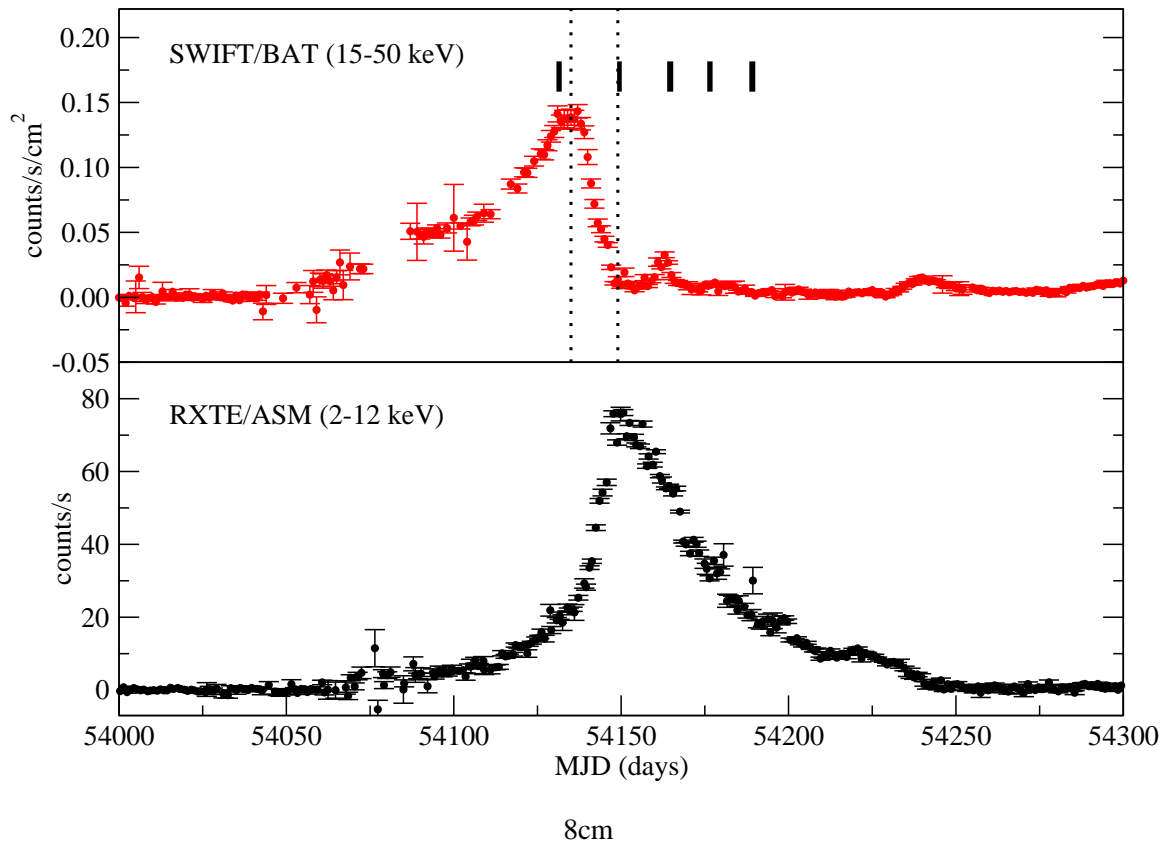


Figure 4: SWIFT/BAT and RXTE/ASM daily light curves of GX 339–4 during the overall outburst in 2007 (red and black dotted lines, respectively), illustrating the spectral evolution between the different states. Intervals of time in which the INTEGRAL observations were undertaken (solid black lines) and the period of time when the radio ejection events were detected (within both dotted black vertical lines) are also shown.

References

- [1] Belloni, T., Homan, J., Casella, P. et al., 2005, *A&A*, 440, 207
- [2] Caballero-García, M. D., Miller, J. M., Díaz Trigo, M., Kuulkers, E., Fabian, A. C., et al., 2008, *ApJ*, accepted (astro-ph/0810.5470)
- [3] Coppi, P. S., 2000, *Bulletin of the American Astronomical Society*, 32, 1217
- [4] Corbel, S., Tzioumis, T., Brocksopp & Fenfer, R., P., 2007, *ATel* 1007
- [5] Esin, A. A., McClintock, J. E. & Narayan, R., 1997, *ApJ*, 489, 865
- [6] Fender, R. P., Belloni, T. M. & Gallo, E., 2004, *MNRAS*, 355, 1105
- [7] Galeev, A. A., Rosner, R. & Vaiana, G. S., 1979, *ApJ*, 229, 318
- [8] George, I. M., Fabian, A. C., 1991, *MNRAS*, 249, 352
- [9] Gierliński, M., Zdziarski, A. A., Poutanen, A. A., et al., 1999, *MNRAS*, 309, 496
- [10] Grove, J. E., Johnson, W. N., Kroeger, R. A., McNaron-Brown, K., Skibo, J. G. & Phlips, B. F., 1998, *ApJ*, 500, 899
- [11] Homan, J., Wijnands, R., van der Klis, M., Belloni, T., van Paradijs, J., Klein-Wolt, M., Fender, R. & Méndez, M., 2001, *ApJS*, 132, 377
- [12] Homan, J., Belloni, T., 2005, *Ap&SS*, 300, 107
- [13] Ibragimov, A. Poutanen, J. Gilfanov, M., et al., 2005, *MNRAS*, 362, 1435
- [14] Joinet, A. Jourdain, E., Malzac, J., Roques, J. P., et al., 2007, *ApJ*, 657, 400
- [15] Laor, A., 1991, *ApJ*, 376, 90
- [16] Maccarone T. J., Coppi P. S., 2003, *MNRAS*, 336, 817
- [17] Malzac, J., Petrucci, P. O., Jourdain, E., et al., 2006, *A&A*, 448, 1125
- [18] Markoff, S., Nowak, M., Corbel, S., Fender, R. & Falcke, H., 2003, *A&A*, 397, 645
- [19] Markoff, S., Nowak, M. A., Wilms, J., 2005, *ApJ*, 635, 1203
- [20] Miller, J. M., Homan, J., Steeghs, D., Rupen, M. et al., 2006, *ApJ*, 653, 525
- [21] Miyamoto S., Kitamoto S., Hayashida K., Egoshi W., 1995, *ApJ*, 442, L13
- [22] Nowak, M. A., Wilms, J. & Dove, J. B., 2002, *MNRAS*, 332, 856
- [23] Rodriguez, J., Shaw, S. E., Hannikainen, D. C., Belloni, T., Corbel, S., Cadolle Bel, M., et al., 2008, *ApJ*, 675, 1449
- [24] Smith D. M., Heindl W. A., Swank J. H., 2002, *ApJ*, 569, 362
- [25] Sunyaev, R. A. & Titarchuk, L., 1980, *A&A*, 86, 121
- [26] Wijnands, R., Homan, J., & van der Klis, M., 1999, *ApJ*, 526L, 33